

Do all stars in the solar neighbourhood form in clusters? A cautionary note on the use of the distribution of surface densities

Mark Gieles, Nickolas Moeckel and Cathie J. Clarke

Institute of Astronomy, University of Cambridge, Madingley Road, Cambridge, CB3 0HA, UK

Accepted 2012 July 09. Received 2012 July 09; in original form 2012 June 24

ABSTRACT

Bressert et al. recently showed that the surface density distribution of low-mass, young stellar objects in the solar neighbourhood is approximately lognormal. The authors conclude that the star formation process is hierarchical and that only a small fraction of stars form in dense star clusters. Here we show that the peak and the width of the density distribution is also what follows if all stars form in bound clusters which are not significantly affected by the presence of gas and expand by two-body relaxation. The peak of the surface density distribution is simply obtained from the typical ages (few Myrs) and cluster membership number (few hundred) typifying nearby star forming regions. This result depends weakly on initial cluster sizes, provided that they are sufficiently dense (initial half mass radius of $\lesssim 0.3$ pc) for dynamical evolution to be important at an age of a few Myrs. We conclude that the degeneracy of the YSO surface density distribution complicates its use as a diagnostic of the stellar formation environment.

Key words: Galaxy: open clusters and associations: general – galaxies: star clusters: – galaxies: stellar content – stars: formation

1 INTRODUCTION

We do not know what fraction of stars form in dense star clusters. Part of the problem is that there is no agreed definitions of what ‘dense’ means and what a star cluster is (Portegies Zwart, McMillan & Gieles 2010). In an attempt to shed light on this situation Bressert et al. (2010) studied a sample of young stellar objects (YSOs) in the solar neighbourhood. They calculate the surface density Σ around each YSO by finding the distance to the 7th nearest neighbour, d_7 , such that $\Sigma = 6/(\pi d_7^2)$. They find that the distribution of Σ is roughly lognormal with a peak at about 22 pc^{-2} and a dispersion of 0.85. Because YSOs are very young (of order 1 Myr) they conclude that this distribution reflects the density distribution at the moment of star formation. They concluded that stars form in a broad and smooth spectrum of surface densities and that only a small fraction of the YSOs form in dense clusters.

In this paper we argue that the observed peak in the surface density distribution of young stars (at around 20 stars per square parsec) is an expected outcome from a wide range of initial clustering configurations. In Section 2 we argue that for ‘typical’ cluster scales in star forming regions ($N \simeq 100$; Lada & Lada 2003) and young ages (about 1 Myr) of YSOs such a surface density represents the outcome of dynamical evolution (i.e. two-body relaxation) from a variety of plausible initial conditions. In Section 3 we flesh out this argument by considering the factors that broaden this distribution (the range of surface densities in a given cluster together with a realistic spectrum of cluster membership number). In Section 4 we present a discussion and conclude that the observed surface density distribution is exactly what one expects if the ma-

jority of stars are born in clusters; the situation is however highly degenerate so that it is not possible to use this distribution to place unique constraints on the initial conditions.

2 THE PEAK OF THE CLUSTER SURFACE DENSITY DISTRIBUTION

The evolution of self-gravitating clusters containing a realistic stellar mass spectrum is well understood. The massive stars segregate to the cluster core due to dynamical drag and initiate core collapse: in the case of clusters numbering a few hundred stars, this occurs after about 10 or 20 crossing times (Giersz & Heggie 1996). Subsequently the cluster expands due to the transfer of energy from binaries and stellar mass-loss in the core by two-body relaxation. This expansion approaches a self-similar state in which the cluster expands more or less homologously and with radius scaling as $t^{2/3}$ (Giersz & Heggie 1996). In this state the two-body relaxation timescale tends to a fixed multiple of the cluster age (Hénon 1965).

Self-gravitating systems are scale free in the sense that, for a given distribution of stars, one can re-scale their spatial separations and not affect their qualitative evolution: in fact, scaling the spatial separations by a factor f simply involves a re-scaling of time by a factor $f^{3/2}$. We illustrate this in Fig. 1 where we show the evolution of the half-mass radius for clusters of 256 stars and with a range of initial radii. It is evident that, although qualitatively identical, the initially compact cluster starts its self-similar expansion earlier. Notably, however, all three clusters are approaching the same self-similar track by an age of a few Myrs.

arXiv:1207.2059v1 [astro-ph.GA] 9 Jul 2012

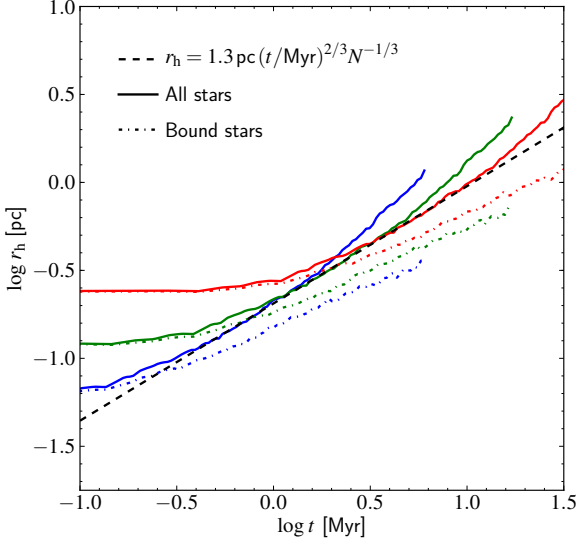


Figure 1. Evolution of the half-mass radii (r_h) of clusters with $N = 256$ in direct N -body integrations with NBODY6 (Aarseth 2003). The stellar mass-function is a Kroupa (2001) distribution between $0.1 M_\odot$ and $100 M_\odot$ and the stars do not evolve internally. The initial positions and velocities were generated from a King (1966) model with $W_0 = 9$. In total 200 simulations were done and the median result for r_h is shown for different initial r_h . The full lines show the result for all the stars and the dashed line for only the bound stars.

Another way to state this is that clusters numbering a hundred stars end up with a mean surface density of around $\lesssim 100 \text{ pc}^{-2}$ at an age of a few Myrs provided they start off with mean densities in excess of that. We therefore deduce that the peak of the surface density distribution observed by Bressert et al. is comparable to what one would expect from dynamical evolution of stellar clusters with ages and richness found in nearby star forming regions (Allen et al. 2007; Gutermuth et al. 2009). We now turn to considering effects which account for the finite width of the distribution, such as the range of cluster membership and the range of surface densities within a given cluster.

3 THE SHAPE OF THE OBSERVED DISTRIBUTION

3.1 Surface density distribution in individual clusters

We start by considering the distribution of surface densities in a single cluster. To facilitate a tractable analytical approach we use a Plummer (1911) model to describe the surface (number) density of the cluster, which has a surface density profile of the form

$$\Sigma(R) = \Sigma_0 \left(1 + \frac{R^2}{R_0^2}\right)^{-2}. \quad (1)$$

Here R is the distance to the centre, R_0 is the scale radius and Σ_0 is the central (and maximum) surface density. The latter depends on the other variables and the total number of stars in the cluster N as $\Sigma_0 = N/(\pi R_0^2)$. The number of stars per logarithmic surface density unit is given by

$$\frac{dn}{d \ln \Sigma} = \Sigma \frac{dn}{dR} \left| \frac{\partial R}{\partial \Sigma(R)} \right|. \quad (2)$$

Using $dn/dR = 2\pi R\Sigma$ and equation (1) we find

$$\frac{dn}{d \ln \Sigma} = \frac{N}{2} \left(\frac{\Sigma}{\Sigma_0} \right)^{1/2}, \quad \Sigma \leq \Sigma_0. \quad (3)$$

If we generalise equation (1) to any cored function with an asymptotic surface density profile with $\Sigma \propto R^{-\gamma}$ then the power-law slope on the right-hand side of equation (3) becomes $1 - \gamma/2$. For the Plummer model $\gamma = 4$, hence we find a logarithmic slope of $1/2$ in equation (3). A shallower profile of $\gamma = 3$ would give a slope of $1/3$. Note that below a surface density of about $N^{-2}\Sigma_0$ the expected number of stars falls to $\lesssim 1$ and we thus have $N^{-2} \lesssim \Sigma/\Sigma_0 \leq 1$. For a cluster with 100 stars there is thus a range of four orders of magnitude in densities. It is interesting to note at this point that the observed spread in densities in YSOs is (only) four orders of magnitude (Bressert et al. 2010). This range is what one gets from a single cluster with $N \simeq 100$ stars. In Fig. 2 we show the Σ distributions for stars in clusters with different N (dashed lines). The sum of the distributions of clusters with different N and Σ_0 gives the overall Σ distribution and we will explain in section 3.2 how this is computed.

3.2 Population of clusters

To get the surface density distribution of all the stars in a population of clusters we need to know the number of clusters with N stars (i.e. the cluster initial mass function, CIMF). We adopt a power-law scaling for the probability that a cluster has between N and $N + dN$ stars with N in the range $N_{\text{low}} \leq N \leq N_{\text{up}}$

$$\phi_{\text{cl}}(N) = A N^{-2}. \quad (4)$$

We can get the total Σ distribution by multiplying $\phi_{\text{cl}}(N)$ by the surface density distribution for the individual clusters (equation 2) and integrating over all clusters,

$$\frac{dn}{d \ln \Sigma} = \int_{N_{\text{low}}}^{N_{\text{up}}} \phi_{\text{cl}}(N) \frac{dn}{d \ln \Sigma} \Big|_{\Sigma_0(N)} dN. \quad (5)$$

To be able to do this, we need to relate the central surface density Σ_0 to the number of stars in the cluster N . Following the arguments of Section 2 we use the size evolution of clusters of a given age in the self-similar regime of cluster expansion. This leads to a solution that is independent of what is assumed for the initial mass-radius relation. In this expansion phase the half-mass relaxation time-scale, τ_{rh} , grows (roughly) linearly with time t (Hénon 1965). A constant ratio of τ_{rh}/t implies $R_0 \propto N^{-1/3} t^{2/3}$ (Spitzer & Hart 1971). Since the cluster expands homologously, the central surface density is proportional to N/R_0^2 and we can thus relate the central surface density Σ_0 to the number of stars in the cluster and the age as

$$\Sigma_0(N, t) = \Sigma_1 \left(\frac{t}{\text{Myr}} \right)^{-4/3} N^{5/3}. \quad (6)$$

Here Σ_1 is a constant of proportionality that is discussed in section 3.3. These relations can now be used to perform a change of variables in equation (5). The result of the integration over Σ_0 is

$$\frac{dn}{d \ln \Sigma} = -\frac{3}{5} A \Sigma^{1/2} \Sigma_0^{-1/2} \Big|_{\Sigma_{0,\text{min}}}^{\Sigma_{0,\text{up}}}, \quad (7)$$

where $\Sigma_{0,\text{up}}$ is the central surface density of the most massive cluster (i.e. $\Sigma_{0,\text{up}} = \Sigma_1 t^{-4/3} N_{\text{up}}^{5/3}$, equation 6) and $\Sigma_{0,\text{min}}$ is

the lower integration boundary. There are two regimes for which different forms for $\Sigma_{0,\min}$ need to be considered. For Σ smaller than the central surface density of the smallest N cluster ($\Sigma < \Sigma_{0,\text{low}} = \Sigma_1 t^{-4/3} N_{\text{low}}^{5/3}$) all clusters contribute to the distribution (see Fig. 2). In this regime $\Sigma_{0,\min} = \Sigma_{0,\text{low}}$. For $\Sigma_{0,\text{low}} < \Sigma \leq \Sigma_{0,\text{up}}$ we need to integrate only over the clusters that contribute to the overall contribution, that is, $\Sigma_{0,\min} = \Sigma$. Using this we find for the surface density distribution of a population of clusters

$$\frac{dn}{d\ln\Sigma} = \frac{3A}{5} \times \begin{cases} \tilde{\Sigma}^{1/2} (\tilde{\Sigma}_{0,\text{low}}^{-1/2} - 1) & , \tilde{\Sigma} < \tilde{\Sigma}_{0,\text{low}}, \\ 1 - \tilde{\Sigma}^{1/2} & , \tilde{\Sigma}_{0,\text{low}} < \tilde{\Sigma} < 1, \end{cases} \quad (8)$$

where tildes denote surface densities normalised to $\Sigma_{0,\text{up}}$.

The distribution has the behaviour of a single cluster (equation 3) at low densities ($\Sigma \leq \Sigma_{0,\text{low}}$). In the regime above $\Sigma_{0,\text{low}}$ (but $\ll \Sigma_{0,\text{up}}$) the distribution is flat: this can be readily understood since the CIMF with -2 contributes equal numbers of stars in equal logarithmic bins of N (and hence, via equation 6, in equal logarithmic bins of $\Sigma(R)$). The peak and width depend on the values of $\Sigma_{0,\text{low}}$ and $\Sigma_{0,\text{up}}$, which both scale with Σ_1 . So what remains to be done is to derive the constant of proportionality in Σ_1 that sets these values.

3.3 Constant of proportionately Σ_1

To complete the model we need to know what the constant of proportionality Σ_1 is in the relation between surface density and age (equation 6). Because we assume a functional form that goes through the origin we thereby also implicitly define the time-scale for clusters to reach the self-similar expansion phase. There are several factors that determine how fast clusters reach the asymptotic track, such as the density profile, the primordial binary star fraction, the amount of primordial mass segregation, the initial virial ratio, etc. Our aim in this section is to find a single value for the constant Σ_1 that is consistent with different numerical results.

We derive the constant of proportionality Σ_1 from the results of two independent sets of N -body simulations of clusters expanding under the influence of two-body relaxation. Note that these models neglect the presence of a gaseous component. This assumption is discussed in section 4. Let us start with the expression for the half-mass radius of an expanding cluster

$$r_h = r_{h,1} \left(\frac{t}{\text{Myr}} \right)^{2/3} N^{-1/3}. \quad (9)$$

From the N -body models shown in Fig. 1 we find that $r_{h,1} = 1.3$ pc. From direct N -body integrations of star clusters with $8192 \leq N \leq 131072$, a full stellar mass-spectrum and including the effect of mass loss of the individual stars, it was found that expansion is important already at an age of a few Myrs for clusters with initial τ_{rh} less than 10 Myr (Gieles et al. 2010). From their Fig. 2 an expansion of $r_h/r_h(0) \simeq 2$ was found at 1 Myr for a cluster with $N = 8192$ and an initial half-mass radius of $r_h(0) \simeq 0.086$ pc (the initial r_h was computed from the mass and initial half-mass density of the cluster). This implies $r_{h,1} \simeq 3.2$ pc. The fact that this value is more than a factor of 2 larger than the estimate from Fig. 1 illustrates that this parameter is quite uncertain. The difference is probably due to the fact that the $N = 8192$ has more massive stars compared to the $N = 256$ cluster, which speeds up the dynamical evolution (Gieles et al. 2010). Moeckel et al. (2012) used direct N -body integrations to evolve

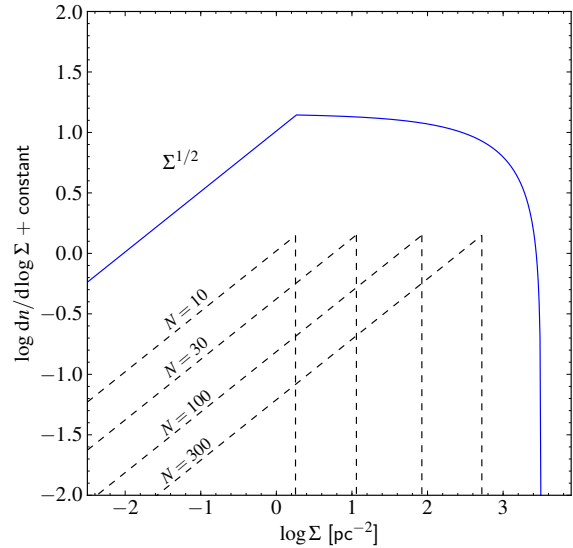


Figure 2. Simple model for the distribution of surface densities around stars. All stars are in clusters that are expanding due to two-body relaxation. The dashed lines show the surface density of the individual clusters with different N (equation 1) weighted by the CIMF. The peak density of each cluster is given by equation (6) and the sum (full line) follows (equations 8) from integrating over the cluster mass function, where we used a -2 power-law distribution between 10 and 500 stars for the clusters (equation 4). An age of 2 Myr was adopted.

small N systems (a few hundred stars) that were selected from the outcome of smoothed particle hydrodynamics (SPH) simulations of a star forming molecular cloud. From their Fig. 12 we derive $1.3 \lesssim r_{h,1}/\text{pc} \lesssim 4.5$. The large variation in $r_{h,1}$ might be because these clusters have undergone varying amounts of dynamical evolution in the hydrodynamical part of the models. Also, these clusters start off with varying degrees of segregation of the massive stars towards the centre.

Having compared the different results, we adopt $r_{h,1} = 2.5$ pc. We are aware that there is an uncertainty of about a factor of two in this value. For a Plummer model the scale radius R_0 is about a factor 1.3 smaller than the half-mass radius. We can then write $\Sigma_1 = (\pi R_0^2)^{-1} \simeq 0.09 \text{ pc}^{-2}$. We use this and equation (6) to find $\Sigma_{0,\text{low}}$ and $\Sigma_{0,\text{up}}$ and to compute the total distribution of Σ using equation (8). The result is shown in Fig. 2 for $t = 2$ Myr. It is not exactly log-normal, but instead asymmetric and skewed towards low densities. This is in fact something that was found in the observations of Bressert et al. (shown in Fig. 3).

The peak, or rather the flat top, of the distribution depends on the density of the average cluster in the CIMF (Fig. 2) and the age of the cluster population. It shifts to lower densities as clusters expand. Therefore, *the location of the peak in this model is insensitive to the details of the mass-size relation of clusters at birth or the densities around the stars when they form.* This is only true if the evolving densities of all clusters have reached the asymptotic $\Sigma_0(N, t)$ relation of equation (6), that is, all clusters must have been denser in the past. In this analytic model the peak is close to the 20 pc^{-2} peak of the observed distribution at an age of 2 Myr. In the next section we make a slightly improved comparison by generating the model in a Monte Carlo fashion.

3.4 Monte Carlo generated model

Fig. 3 shows a direct comparison between a Monte Carlo generated sample of our model (points with error bars) to the result for the total of the three Spitzer surveys of young stellar objects (YSOs) (histogram) used in Bressert et al. (2010). All distributions are normalised to an area of unity.

Each cluster population contains 10 clusters with the number of stars in the cluster randomly drawn from the mass-function of equation (4) with $N_{\text{low}} = 50$ and $N_{\text{up}} = 500$. This results in an average of roughly 10^3 stars in each cluster population, which is similar to the total number of sources in the individual surveys considered by Bressert et al. (2010). Note that the Orion Nebula Cluster (ONC) is excluded from their Orion sample and an upper limit of a few hundred stars is, therefore, probably appropriate for the Solar neighbourhood minus the ONC. For each star the surface density is determined by finding the distance to the 7th nearest neighbour as was done for the observations (section 1). An age of 2 Myr is adopted. We generate 1000 cluster populations and show the median values and the boundaries containing 67% of the points around the median as circles and error bars, respectively. The (blue) solid line shows the analytical result of section 3.2.

The peak values of the simulated distributions are remarkably close to the observed peak. We also show the analytical model results for ages of 1 Myr and 4 Myr, to show how the peak evolves in time. Bressert et al. (2010) find a small offset in the density distributions of the class I and the class II objects, with the class II objects being slightly less dense. Because class II objects are older this could thus be interpreted as dynamical evolution (i.e. expansion)¹. There are several physical effects we do not consider here, such as the effects of multiple overlapping clusters and the effects of the presence of gas on the cluster dynamics. Although it is not our aim to develop a model that reproduces the observations in detail we discuss what the effect of the presence of gas could be in the next section.

4 DISCUSSION AND CONCLUSIONS

We showed that the distribution of surface densities of YSOs presented by Bressert et al. (2010), that was used to argue that only a small fraction of the stars form in dense clusters, can be reproduced by an extremely simple model in which all stars form in dense star clusters. In this model the location of the peak of the distribution is a measure of the age of the cluster population and the typical membership number of young clusters. Our model requires the clusters to form with higher densities than they have at the present day, which is a constraint on the physics of the star formation process which can be tested with future facilities, such as ALMA.

There are several physical effects that we have not included, such as the details of the spatial distribution of YSO on the sky and the presence of gas. Although it is beyond the scope of this work to present realistic models that include all these effects, it may be interesting to discuss the omission of gas in our modelling in a bit more detail. This is motivated by the observation that YSOs trace the molecular gas they form from and the total gas mass in star forming regions can be 10 or 20 times the total mass in YSOs (e.g. Kennicutt & Evans 2012), with average gas surface (mass) densities

¹ Bressert et al. consider this but conclude, in fact, that the similarity between the distribution of the class I and class II objects supports their assumption that the spatial distribution of YSOs is primordial.

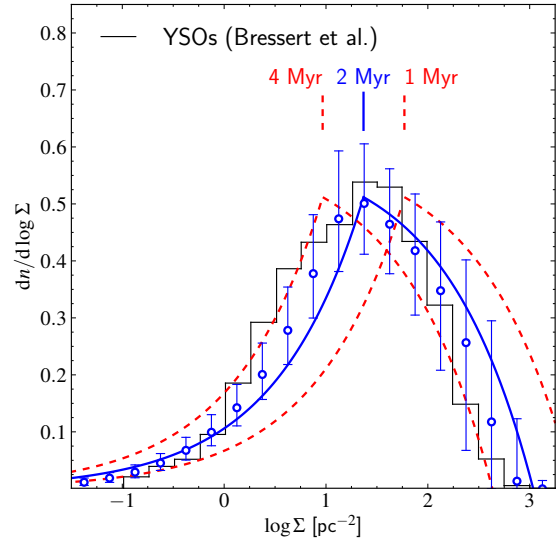


Figure 3. Surface density distribution of YSOs (histogram) as found from the surveys used by Bressert et al. (2010). Results of the Monte Carlo simulations using $50 \leq N \leq 500$ are shown as open (blue) circles with error bars. The (blue) solid line shows the analytical model of section 3.2 for an age of 2 Myr, whereas the (red) dashed lines show the results for ages of 1 and 4 Myr. To conform with Bressert et al.’s figure we plot $dn/d \log \Sigma$ rather than $\log(dn/d \log \Sigma)$ as in Figure 2. All distributions are normalised to unit area.

three or four times the surface (mass) density of YSOs (Gutermuth et al. 2009).

A star cluster embedded in an external potential (e.g. gas) will have a higher velocity dispersion, which slows down the two-body relaxation that causes the expansion we discuss here. This is because τ_{rh} depends on the stellar velocity dispersion σ and the stellar density ρ as $\tau_{\text{rh}} \propto \sigma^3/\rho$ (Spitzer & Hart 1971). To estimate the contribution to σ of the gas we assume two spherically symmetric distributions, with the same functional form for the density profile. Using r_{h} and $r_{\text{h,g}}$ for the half-mass radii of the stellar and gaseous component, respectively, and M and M_{g} for the corresponding total masses. The velocity dispersion of the stars can then be expressed in the stellar and gas parameters as (Spitzer 1969)

$$\sigma^2 \propto \frac{GM}{r_{\text{h}}} \left(1 + \frac{M_{\text{g}}}{M} \frac{r_{\text{h}}^3}{r_{\text{h,g}}^3} \right). \quad (10)$$

The first term on the right-hand side is due to self-gravity of the stars and the second term is the contribution of the gas. If the gas and stellar distribution have the same half-mass radius then we find $\sigma^2 \propto (M + M_{\text{g}})/r_{\text{h}}$, which is what is usually assumed for models that consider the removal of natal gas from an embedded cluster. Introducing $\eta = M_{\text{g}}/M$ and $\mu = r_{\text{h,g}}/r_{\text{h}}$ we can compare the relaxation time-scale of a gas embedded system to that of a system containing only stars (i.e. what is assumed here)

$$\tau_{\text{rh}}(\text{stars and gas}) = \left(1 + \frac{\eta}{\mu^3} \right)^{3/2} \tau_{\text{rh}}(\text{stars}). \quad (11)$$

From this we see that τ_{rh} of a gas embedded system is longer if a significant amount of gas is present ($\eta \gtrsim 1$) which has a compara-

ble half-mass radius ($\mu \simeq 1$). But the increase of τ_{rh} depends sensitively on the size of the gaseous system in which the stars evolve (a μ^{-3} dependence), so the effect of an additional gas component becomes negligible if $\mu \gtrsim 3$. Note that η/μ^3 is the ratio of the (volume) densities of the stars and the gas within their half-mass radii. This is not the same as the local (volume) density contrast. Estimates of η and (surface) density contrasts are available in some dense embedded clusters but it is not trivial to estimate the value of μ from these observations. If $\mu \simeq 1$ the effect of dynamical expansion can be overestimated by an order of magnitude. On the other hand, if $\mu \gtrsim 3$, our assumption of gas free cluster evolution is justified.

From SPH simulations it was found that gas dominated star forming regions are in fact gas-poor on the scale of the (sink) particles (i.e. $\mu \gg 1$, Moeckel et al. 2012). Arguments as to why this might happen can be found in Kruijssen et al. (2012). Similar results were obtained from adaptive mesh refinement (AMR) simulations (Girichidis et al. 2012). The results of these numerical studies support our assumption of pure stellar dynamical evolution.

We conclude that the distribution of surface densities can not be used as evidence that not all stars form in dense clusters. Similarly, the agreement between this model and the observations should not be construed as an argument that *all* stars necessarily form in clusters. Bressert et al. (2010) argue that a (roughly) log-normal density distribution is evidence against a scenario in which stars form in distinct ‘clustered’ and ‘distributed’ star formation modes. Their argument is that the distribution would be bi-modal (or multi-modal) if there were distinct modes. However, if we interpret the model in Fig. 3 as a ‘clustered’ star formation mode, we can add a ‘distributed’ mode with a density of several tens of YSOs per pc^2 and some dispersion and the total distribution would still be unimodal. Our results support the suggestion of Bressert et al. (2010) that a (local) surface density threshold is not a useful tool to separate clusters from field stars, because in our model all stars are in clusters and there is a range of about four orders of magnitude in surface density.

ACKNOWLEDGEMENT

We thank Thomas Maschberger for interesting discussions and Eli Bressert and Nate Bastian for comments on earlier versions of the manuscript. We also thank Simon Goodwin for a constructive referee report. MG acknowledges financial support from the Royal Society.

REFERENCES

- Aarseth S. J., 2003, *Gravitational N-Body Simulations*. Cambridge University Press, November 2003.
- Allen L., Megeath S. T., Gutermuth R., Myers P. C., Wolk S., Adams F. C., Muzerolle J., Young E., Pipher J. L., 2007, *Protostars and Planets V*, pp 361–376
- Bressert E., Bastian N., Gutermuth R., Megeath S. T., Allen L., Evans II N. J., Rebull L. M., Hatchell J., Johnstone D., Bourke T. L., Cieza L. A., Harvey P. M., Merin B., Ray T. P., Tothill N. F. H., 2010, *MNRAS*, 409, L54
- Gieles M., Baumgardt H., Heggie D. C., Lamers H. J. G. L. M., 2010, *MNRAS*, 408, L16
- Giersz M., Heggie D. C., 1996, *MNRAS*, 279, 1037
- Girichidis P., Federrath C., Allison R., Banerjee R., Klessen R. S., 2012, *MNRAS*, 420, 3264
- Gutermuth R. A., Megeath S. T., Myers P. C., Allen L. E., Pipher J. L., Fazio G. G., 2009, *ApJS*, 184, 18
- Hénon M., 1965, *Annales d’Astrophysique*, 28, 62
- Kennicutt Jr R. C., Evans II N. J., 2012, arXiv:1204.3552
- King I. R., 1966, *AJ*, 71, 64
- Kroupa P., 2001, *MNRAS*, 322, 231
- Kruijssen J. M. D., Maschberger T., Moeckel N., Clarke C. J., Bastian N., Bonnell I. A., 2012, *MNRAS*, 419, 841
- Moeckel N., Holland C., Clarke C. J., Bonnell I. A., 2012, *MNRAS*, in press (arXiv:1205.1677)
- Plummer H. C., 1911, *MNRAS*, 71, 460
- Portegies Zwart S. F., McMillan S. L. W., Gieles M., 2010, *ARA&A*, 48, 431
- Spitzer L. J., 1969, *ApJ*, 158, L139
- Spitzer L. J., Hart M. H., 1971, *ApJ*, 164, 399